

# OSTEOPOROSIS PRESCREENING USING DENTAL PANORAMIC RADIOGRAPHS FEATURE ANALYSIS

Chunjuan Bo<sup>a,b</sup>, Xin Liang<sup>c</sup>, Peng Chu<sup>b</sup>, Jonathan Xu<sup>b</sup>, Dong Wang<sup>b,d</sup>, Jie Yang<sup>e</sup>, Vasileios Megalooikonomou<sup>b,f</sup>, Haibin Ling<sup>b\*</sup>

<sup>a</sup>College of Electromechanical Engineering, Dalian Nationalities University, Dalian, China

<sup>b</sup>Department of Computer and Information Science, Temple University, Philadelphia, USA

<sup>c</sup>School of Stomatology, Dalian Medical University, Dalian, China

<sup>d</sup>School of Information and Communication Engineering, Dalian University of Technology, Dalian, China

<sup>e</sup>Division of Oral and Maxillofacial Radiology, School of Dentistry, Temple University, Philadelphia, USA

<sup>f</sup>Computer Engineering and Informatics Department, University of Patras, Patras, Greece

## ABSTRACT

A panoramic radiography image provides not only details of teeth but also rich information about trabecular bone. Recent studies have addressed the correlation between trabecular bone structure and osteoporosis. In this paper, we collect a dataset containing 40 images from 40 different subjects, and construct a new methodology based on a two-stage classification framework that combines multiple trabecular bone regions of interest (ROIs) for osteoporosis prescreening. In the first stage, different support vector machines (SVMs) are adopted to describe different information of different ROIs. In the second stage, the output probabilities of the first stage are effectively combined by using an additional linear SVM model to make a final prediction. Based on our two stage model, we test the performance of different image features by using leave-one-out cross-valuation and analysis of variance rules. The results suggest that the proposed method with the HOG (histogram of oriented gradients) feature achieves the best overall accuracy.

**Index Terms**— Osteoporosis; Panoramic Radiography; Image Features; Support Vector Machine; Two-Stage Model.

## 1. INTRODUCTION

Osteoporosis is a disease where decreased bone strength increases the risk of a broken bone [1]. Usually, osteoporosis is diagnosed by bone mineral density (BMD) measurements (expressed as a T-score), and dual-energy x-ray absorptiometry (DXA) is considered as the reference-standard examination for BMD assessment. But this technique is expensive and has a limited availability in population diagnosing [2].

Compared with DXA, panoramic radiography is a relatively inexpensive and convenient screening method for selecting high-risk osteoporosis patients [3]. Many research works have demonstrated the feasibility of BMD estimation

and osteoporosis diagnosis by using panoramic radiography [4–8]. In [9], Honer *et al.* investigated the relationship between DXA measurements and some densitometric and linear measurements including mandibular cortical thickness (MCT) and panoramic mandibular index (PMI). The experimental results show that the MCT value is significantly correlated with mandibular BMD but the later index is not suitable for osteoporosis diagnosis. In [10] and [11], the correlations of several panoramic radiomorphometric indices with lumbar spine and hip BMDs have been verified, which also demonstrates that the mental index, mandibular cortical index and visual estimation of cortical width are more accurate indices and can be used as osteoporosis predictors. Although those studies provide sufficient evidence for assisting osteoporosis diagnosis via panoramic radiograph, they have not investigated the roles of the image features (such as intensity, texture, and others) for diagnosing osteoporosis.

Image feature information of trabecular bone has been known to be correlated closely to bone density change and therefore can be used to help the evaluation of osteoporosis. In the last decades, the relationship between trabecular bone structure and osteoporosis has been presented in a variety of biomedical contexts. In 1983, Parfitt *et al.* [12] introduced the importance of trabecular perforations in the development of osteoporosis and revealed that the change of the trabecular bone texture in iliac can foresee osteoporosis based on its surface texture, volume and thickness. Eriksen explained the relation between the profound disintegration of the trabecular network and certain bone diseases [13]. Faber *et al.* [14] exploited Fourier and wavelet analyses to detect trabecular changes in osteoporosis, showing that the Fourier analysis is more suitable for subject classification than the wavelet analysis. Tosoni *et al.* [15] compared the pixel intensity values and fractal dimensions in some selected mandibular regions and demonstrated that the pixel intensity measurements are significantly correlated with osteoporosis. Ling *et al.* [16] investigated the correlation between various CBCT features

---

Correspondence author.

and gender-age groups, which implicitly relate to bone quality changes. Inspired by these studies, Li *et al.* [17] presented a generalized multiple kernel learning framework to fuse different texture features from multiple regions of interest, and the framework was applied to gender-age group separation and therefore has the potential for bone-quality assessment.

To the best of our knowledge, there exists no effective automatic osteoporosis classification method for the panoramic radiography images based on trabecular feature analysis. This paper proposes an osteoporosis decision making assistance method based on panoramic radiographs feature analysis. More specifically, we exploit a two-stage classification framework to combine the image features from multi-ROIs in panoramic radiography images. In the first stage, different support vector machine (SVM) models are adopted to describe the feature information of different ROIs. In the second stage, an additional SVM model is exploited to effectively combine the output probabilities of the first stage and then to conduct a final decision.

## 2. DATA AND METHODOLOGY

### 2.1. DPR Image and Multiple Dental ROIs

Dental panoramic radiography (DPR) is a two-dimensional dental x-ray examination, which is able to capture the entire mouth in a single image (including the teeth, upper and lower jaws, surrounding structures and tissues). The DPR image not only provides a relatively convenient and cheap way for aiding teeth problem diagnosis and treatment planning, but also includes rich information about trabecular bone structure that can be used to study the osteoporosis problem.

In order to study osteoporosis based on DPR, we collected a dataset containing 40 images from 40 different subjects, including 19 subjects with osteoporosis and 21 subjects without osteoporosis (i.e., normal persons). The subjects was classified according to the World Health Organization [18] as normal (T-score  $\geq -1.0$ ) or osteoporotic (T-score  $\leq -2.5$ ). Each DPR scan was obtained by using a orthophos XG5 (sirona) machine. Benefiting from the fact that trabecular patterns are distributed in various places in the oral cavity, in this work we integrated information from multiple ROIs for robustness. In each panoramic radiography image, we exploited eight ROIs illustrated in Figure 1 (each ROI is normalized into  $50 \times 50$  pixels), and then divided them into four groups (Group 1: ROIs 1, 2; Group 2: ROIs 3, 4; Group 3: ROIs 5, 6; and Group 4: ROIs 7, 8) due to symmetry.

### 2.2. Feature Descriptors

In order to analyze osteoporosis conditions, we firstly extract different types of feature descriptors from each panoramic image. Each image has 8 ROIs that are divided into 4 groups (defined above). For each group, two feature vectors are extracted and concatenated into a long vector. In

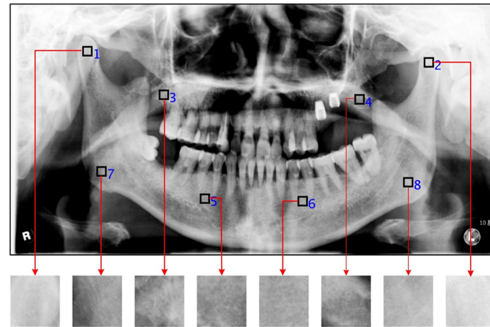


**Fig. 1.** A panoramic radiography image with eight manually annotated ROIs. The physical meanings of the eight ROIs are as follows: 1(2). condylar right (left); 3(4). maxillar molar region right (left); 5(6). mandibular premolar region right (left); and 7(8). mandibular angle right (left).

this work, three types of features are adopted, i.e., intensity histogram, local binary pattern histogram and histogram of oriented gradient descriptor.

**Intensity Histogram:** The intensity histogram is a very commonly used feature in image processing, which is a graph indicating the number of pixels in an image at different intensity ranges. For extracting the intensity histogram in each ROI, we first divide the entire intensity range of values into a series of intervals and then count how many values fall into each interval. After that, the histogram is normalized to reflect the underlying intensity distribution.

**LBP Histogram:** The local binary pattern (LBP) operator was first introduced by Ojala *et al.* [19]. It simply labels image pixels by thresholding the  $3 \times 3$  neighborhood of each pixel with the center intensity and resulting in a binary value. There are two major advantages on LBP features: (1) it is computationally efficient since the LBP operator can be implemented as a few operations in a small neighborhood with a lookup table; (2) it is robust against gray-scale variations since the LBP operator explicitly takes gray-scale monotonic transformation into consideration. Later, Ojala *et al.* [20] conducted two critical extensions for the original LBP operator, i.e., “uniform” patterns and “ $P, R$ ” operators. The definition of “uniform” patterns is able to make the LBP operator maintain a vast majority of local texture patterns and at the same time reduce feature dimension. The latter one,  $LBP_{P,R}$ , produces  $2^P$  different binary patterns corresponding to  $P$  pixels in the neighbor set with radius  $R$ . In this work, we first adopt the standard  $LBP_{P,R}^{u2}$  operator to extract LBP texture features for each ROI (the superscript  $u2$  stands for using only uniform patterns and considering all remaining patterns as a single label). Then, the normalized histogram technique is employed to exploit the LBP histogram.

**HOG Descriptor:** The histogram of oriented gradients (HOG) [21, 22] is an effective feature descriptor used in image processing for dealing with detection and classification problems. For a ROI, the HOG operator is able to describe the

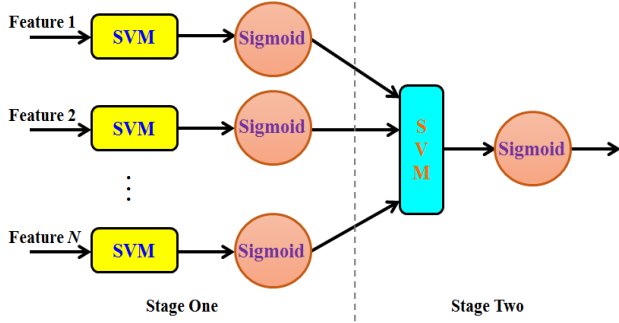


Fig. 2. The framework of our two-stage classification model.

local shape information by a histogram of edge orientations. The contributions of different edges are weighted according to their gradient magnitude. For each ROI, the HOG descriptor can be extracted based on the following steps: (a) calculate the gradient magnitudes and directions for all pixels within the image region; (b) discretize each pixel into angular bins according to its orientation; (c) make histogram statistics by accumulating the gradient magnitude of each pixel into its corresponding angular bin; and (d) normalize the histogram to obtain the final HOG descriptor.

### 2.3. Two-stage Classification Framework

In this work, we exploit a two-stage classification framework to combine four groups of ROIs for a given feature. The flowchart of our classification framework is illustrated in Figure 2. First, each individual classifier is trained based on its corresponding ROI group for a given feature (intensity, LBP or HOG). Here, we use  $\mathbf{c}_i, i = 1, 2, \dots, 4$  to denote the feature representation of  $i$ -th group in each DPR image. For the  $i$ -th group, we train a corresponding linear SVM model  $f_i^1(\mathbf{c}_i)$ , where the superscript denotes the SVM model in the first stage and the subscript  $i$  denotes the  $i$ -th ROI group.

Then, the classification outputs  $f_i^1(\mathbf{c}_i), i = 1, 2, \dots, 4$  are converted to the probability outputs by using the sigmoid function, i.e.,

$$p_i^1(l_i = 1|\mathbf{c}_i) = \frac{1}{1 + \exp[-f_i^1(\mathbf{c}_i)]}. \quad (1)$$

By treating  $\mathbf{p} = [p_1^1(l_1 = 1|\mathbf{c}_1), \dots, p_4^1(l_4 = 1|\mathbf{c}_4)]^\top$  as a meta-feature, an additional linear SVM  $f^2(\cdot)$  is trained to combine different cues inspired by the learning-based ensemble idea [23]. We note that the penalty factors of all SVM models are set to 500 in this work.

Finally, the sigmoid function is applied to convert the output of the second stage into a probability, which also can be viewed as a kind of an osteoporosis index.

## 3. EXPERIMENTS AND RESULTS

### 3.1. Evaluation Criteria

**Leave-one-out cross-validation (LOOCV):** LOOCV is a simple cross-validation technique, in which each training set is constructed by taking all samples except one and the corresponding test set is the sample left out. To be specific, for  $n$  samples, we have  $n$  different training and test sets. Thus, the LOOCV accuracy that is calculated by averaging the  $n$  classification outputs is used to evaluate the performance of different classification methods. Specifically, we adopt three criteria to measure the performance of a given algorithm, including overall accuracy (OA), osteoporosis accuracy (OPA) and non-osteoporosis accuracy (NOPA)<sup>1</sup>.

**Analysis of variance (ANOVA):** Statistical analysis is usually adopted to verify the effectiveness of output indices in medical image analysis. In this work, we conduct ANOVA based on the two-sample  $t$ -test, and report the  $p$ -value for the  $t$ -test in the following experiments.

### 3.2. Overall classification performance with different feature parameters

First, we investigate the effect of the number of bins for intensity histogram features in Table 1. We can see from Table 1 that the intensity histogram with 16 bins achieves a better performance. Second, we attempt the commonly used parameters ( $P = 8, 16$  and  $R = 1, 2$ ) for the LBP features. It can be seen from Table 2 that the  $LBP_{16,1}$  descriptor achieves the best result. Finally, Table 3 demonstrates that the classification model with the HOG feature achieves a stable result when the number of bins is around 64. The best results are denoted by the red color in every row for all three tables.

Table 1. Classification results using intensity histogram with various numbers of bins.

#Bins	8	16	24	48	64	80
OA(%)	42.50	55.00	55.00	55.00	52.50	50.00
NOPA(%)	47.62	52.63	66.67	57.14	52.38	61.90
OPA(%)	36.84	63.16	42.11	52.63	52.63	36.84
$p$ -value	0.3257	0.138	0.2190	0.8299	0.6167	0.8495

Table 2. Classification results using LBP with various parameter configurations

$P, R$	8, 1	8, 2	16, 1	16, 2
OA(%)	60.00	62.50	57.50	65.00
NOPA(%)	61.90	61.90	61.90	80.95
OPA(%)	57.89	63.16	52.63	47.37
$p$ -value	0.1654	0.0509	0.2623	0.0029

<sup>1</sup>OA is defined as the ratio of correctly classified samples to all samples. OPA is calculated as the ratio of correctly classified samples with osteoporosis to all osteoporosis samples, and NOPA is computed as the ratio of correctly classified non-osteoporosis samples to all non-osteoporosis samples.

**Table 3.** Classification results using HOG with various numbers of bins

#Bins	8	16	24	48	64	80
OA(%)	45.00	45.00	47.50	55.00	<b>72.50</b>	57.50
NOPA(%)	42.86	38.10	33.33	52.38	<b>71.43</b>	66.67
OPA(%)	47.37	52.63	63.16	57.89	<b>73.68</b>	47.37
<i>p</i> -value	0.2509	0.6063	0.6275	0.3482	<b>0.0164</b>	0.3022

#### 4. CONCLUSION

In this paper, we used a dental panoramic radiography dataset for studying the osteoporosis problem and proposed an image-based osteoporosis classification method. The proposed method combines multi-ROI information by using a two-stage classification model. In the first stage, each linear SVM model is constructed with respect to a given feature and a grouped region. The probability outputs of the first stage SVM models are combined by using a new SVM model. The experimental results show that our method with the HOG feature achieves the best overall accuracy of 72.5% with a relatively low *p*-value (0.0164). Thus, we note that the combination of machine learning techniques and image feature analysis on panoramic radiography images has some potential for osteoporosis prescreening. In the further, we will collect more data and exploit more effective features to improve the classification performance. We will also attempt to develop a method to automatically annotate the ROIs.

ACKNOWLEDGEMENTS. This work was supported in part by NSF Research Grants 1407156 and IIS-1350521.

#### 5. REFERENCES

- [1] A.L. Golob and M.B. Laya, "Osteoporosis: screening, prevention, and management," *Medical Clinics of North America*, vol. 99, no. 3, pp. 587–606, 2015.
- [2] J.A. Kanis and O. Johnell, "Requirements for DXA for the management of osteoporosis in europe," *Bone*, vol. 16, no. 3, pp. 229–238, 2005.
- [3] A. Taguchia, A. Asanob, M. Ohtsukac, T. Nakamotoc, Y. Sueia, M. Tsudad, Y. Kudod, K. Inagakie, T. Noguchie, K. Tanimotoc, R. Jacobsf, E. Klemettig, S.C. Whiteh, and K. Horneri, "Observer performance in diagnosing osteoporosis by dental panoramic radiographs: results from the osteoporosis screening project in dentistry (OSPD)," *Bone*, vol. 43, no. 1, pp. 209–213, 2008.
- [4] W.G.M. Geraetsa, J.G.C. Verheijja, P.F. van der Stelta, K. Hornerb, C. Lindhc, K. Nicopoulou-Karayiannid, R. Jacobse, E.J. Harrisonf, J.E. Adamsf, and H. Devlinb, "Prediction of bone mineral density with dental radiographs," *Bone*, vol. 40, no. 5, pp. 1217–1221, 2007.
- [5] H. Devlin, K. Karayianni, A. Mitsea, R. Jacobs, C. Lindh, P. van der Stelt, E. Marjanovic, J. Adams, S. Pavitt, and K. Horner, "Diagnosing osteoporosis by using dental panoramic radiographs: The OSTEO-DENT project," *Oral Surgery, Oral Medicine, Oral Pathology, Oral Radiology and Endodontology*, vol. 104, no. 6, pp. 821–828, 2007.
- [6] B. Cakur, A. Sahin, S. Dagistan, O. Altun, F. Caglayan, O. Miloglu, and A. Harorli, "Dental panoramic radiography in the diagnosis of osteoporosis," *Journal of International Medical Research*, vol. 36, no. 4, pp. 792–799, 2008.
- [7] A. Taguchi, "Panoramic radiographs for identifying individuals with undetected osteoporosis," *Japanese Dental Science Review*, vol. 45, no. 2, pp. 109–120, 2009.
- [8] M. Boi and N.I. Hren, "A novel method of dental panoramic tomogram analysis: A perspective tool for a screening test for osteoporosis," *Journal of Cranio-Maxillofacial Surgery*, vol. 41, no. 8, pp. 808–815, 2013.
- [9] K. Horner and H. Devlin, "The relationship between mandibular bone mineral density and panoramic radiographic measurements," *Journal of Dentistry*, vol. 26, no. 4, pp. 337–343, 1998.
- [10] K.Z. Vlasidisa, C.A. Skouterisb, G.A. Velegrakisc, I. Fragoulid, J.M. Neratzoulakise, J. Damilakisf, and E.E. Koumantakisg, "Mandibular radiomorphometric measurements as indicators of possible osteoporosis in postmenopausal women," *Maturitas*, vol. 58, no. 3, pp. 226–235, 2007.
- [11] A.F. Leite, P.T. de Souza Figueiredo, C.M. Guia, N.S. Melo, and A.P. de Paula, "Correlations between seven panoramic radiomorphometric indices and bone mineral density in postmenopausal women," *Oral Surgery, Oral Medicine, Oral Pathology, Oral Radiology, and Endodontology*, vol. 109, no. 3, pp. 1734–1742, 2010.
- [12] A.M. Parfitt, C.H. Mathews, A.R. Villanueva, M. Kleerekoper, B. Frame, and D.S. Rao, "Relationships between surface, volume, and thickness of iliac trabecular bone in aging and in osteoporosis," *Journal of Clinical Investigation*, vol. 72, no. 4, pp. 1396–1409, 1983.
- [13] E.F. Eriksen, "Normal and pathological remodeling of human trabecular bone: three dimensional reconstruction of the remodeling sequence in normals and in metabolic bone disease," *Endocrine Reviews*, vol. 7, no. 4, pp. 379–408, 1996.
- [14] T.D. Faber, D.C. Yoon, S.K. Service, and S.C. White, "Fourier and wavelet analyses of dental radiographs detect trabecular changes in osteoporosis," *Bone*, vol. 35, no. 2, pp. 403–411, 2004.
- [15] G.M. Tosoni, A.G. Lurie, A.E. Cowan, and J.A. Burleson, "Pixel intensity and fractal analyses: detecting osteoporosis in perimenopausal and postmenopausal women by using digital panoramic imagesoriginal," *Oral Surgery, Oral Medicine, Oral Pathology, Oral Radiology, and Endodontology*, vol. 102, no. 2, pp. 235–241, 2006.
- [16] H. Ling, X. Yang, P. Li andn V. Megalooikonomou, Y. Xu, and J. Yang, "Cross gender-age trabecular texture analysis in dental cone beam computed tomography," *Dentomaxillofacial Radiology*, vol. 43, pp. 20130324, 2014.
- [17] P. Li, X. Yang, F. Xie, J. Yang, E. Cheng, V. Megalooikonomou, Y. Xu, and H. Ling, "Trabecular texture analysis in dental CBCT by multi-roi multi-feature fusion," in *In Proc. of IEEE Int'l Symposium on Biomedical Imaging*, 2014, pp. 846–849.
- [18] H. Orimo, Y. Hayashi, M. Fukunaga, T. Sone, S. Fujiwara, M. Shiraki, K. Kushida, S. Miyamoto, S. Soen, J. Nishimura, Y. Oh-Hashi, T. Hosoi, I. Gorai, H. Tanaka, T. Igai, and H. Kishimoto, "Diagnostic efficacy of panoramic radiography in detection of osteoporosis in post-menopausal women with low bone mineral density," *Diagnostic criteria for primary osteoporosis: year 2000 revision*, vol. 19, no. 6, 2001.
- [19] T. Ojala, M. Pietikäinen, and D. Harwood, "A comparative study of texture measures with classification based on featured distributions," *Pattern Recognition*, vol. 29, no. 1, pp. 51–59, 1996.
- [20] T. Ojala, M. Pietikäinen, and T. Mäenpää, "Multiresolution gray-scale and rotation invariant texture classification with local binary patterns," *IEEE Transactions on Pattern Analysis and Machine Intelligence*, vol. 24, no. 7, pp. 971–987, 2002.
- [21] N. Dalal and B. Triggs, "Histograms of oriented gradients for human detection," in *In Proc. of IEEE Conf. on Computer Vision and Pattern Recognition*, 2005, pp. 886–893.
- [22] C. Vondrick, A. Khosla, T. Malisiewicz, and A. Torralba, "Hoggles: Visualizing object detection features," in *In Proc. of IEEE Int'l Conf. on Computer Vision*, 2013, pp. 1–8.
- [23] R. Polikar, "Ensemble based systems in decision making," *IEEE Circuits and Systems Magazine*, vol. 6, no. 3, pp. 21–45, 2006.